The cleavage furrow ingression and cell separation are both accompanied by calcium spikes during fission yeast cytokinesis

Abhishek Poddar[1], Oumou Sidibe[1], and Qian Chen[1]*

* Correspondence: qian.chen3@utoledo.edu

[1]: Department of Biological Sciences

The University of Toledo

2801 West Bancroft ST

Toledo, OH, 43606

Running title: Calcium spikes during yeast cytokinesis.

Abbreviations:

Keyword: cytokinesis, calcium transient, fission yeast, GCaMP

Abstract

The role of calcium during cell division has long remained ambiguous. The intracellular calcium concentration of many animal embryos increases transiently during cytokinesis, leading to the long-standing proposal that calcium transients may trigger the contraction of actomyosin ring. However, it remains unknown whether these calcium transients can be found in cells beyond those large embryos and whether they have any role in cytokinesis. Here we addressed these questions in the unicellular model organism fission yeast by adopting GCaMP, a genetically encoded indicator, to determine its intracellular calcium level. With confocal microscopy, we captured both the calcium homeostasis and the calcium transients in live cells using this calcium reporter. We searched for the cytokinetic calcium transients using two independent approaches. Both analyses of the intracellular calcium in a population and time-lapse microscopy of dividing cell revealed two cytokinetic calcium spikes. The first initiated at the beginning of the cleavage furrow ingression and the second one at the end of the cell separation. The temporal regulation of these spikes bears a strong similarity to the two calcium waves discovered in the cytokinesis of fish embryos. These slow calcium spikes propagated intracellularly, not restricted to the cell division plane. Although depletion of these spikes did not prevent the contractile ring from contracting as predicted, it reduced the rate of contraction and led to lysis of many daughter cells. We conclude that the fission yeast cytokinetic calcium spikes promote the contractile ring closure and the integrity of separating cells, but they are not required for triggering the ring contraction. Our discovery suggests that transient increase of intracellular calcium may be a conserved regulatory mechanism of cytokinesis among eukaryotes.

Introduction

Calcium is an essential secondary messenger in many cellular processes but its role during

cytokinesis, the last stage of cell division, remains ambiguous. Eukaryotic cells maintain their intracellular calcium at much lower concentration than that of the extracellular environment. A transient increase of the calcium level, through either release from the intracellular storage or influx through the plasma membrane, triggers a number of important signaling pathways (for a review see (Clapham, 2007)). Although the importance of calcium to cytokinesis had long been confirmed (Arnold, 1975), the calcium transients accompanying cytokinesis were discovered much later (Fluck et al., 1991). Two localized calcium waves, restricted to the cell division plane, initiate at the time of cleavage furrow ingression and after the cell separation respectively. A similar transient and localized increase of calcium was also discovered in other animal embryos including those of zebra fish *Danio rerio* and African frog *Xenopus laevis* (Chang and Meng, 1995a; Miller et al., 1993; Noguchi and Mabuchi, 2002). What remains unclear is whether such calcium transients are universal among all eukaryotic cells. Neither is there a consensus on the exact molecular role and significance of these transients. The prevailing hypothesis (Chang and Meng, 1995b; Fluck et al., 1991) is that the increase of free intracellular calcium activates myosin light chain kinase (MLCK) which could in turn activate myosin II and trigger contraction of the contractile ring (Craig et al., 1983; Scholey et al., 1980). This proposed mechanism bears a strong similarity to how calcium triggers the smooth muscle contraction (Nishimura et al., 1990). However, it has remained far from proven even in the animal embryos. Adding to the ambiguity, inhibition of the cytokinetic calcium transients in *X. laevis* embryos has produced conflicting results (Miller et al., 1993; Noguchi and Mabuchi, 2002; Snow and Nuccitelli, 1993). To date, both the nature and molecular function of the cytokinetic calcium transients remain unclear far from clear.

Fission yeast *Schizosacchromyces pombe* is an excellent model organism for studying

cytokinesis. Its molecular mechanism of cytokinesis has been largely conserved in higher eukaryotes (for review see (Pollard and Wu, 2010)). Like animal cells, fission yeast assembles an actomyosin contractile ring at the cell division plane (Wu et al., 2003), a process mediated by essential cytokinetic proteins such as Myo2p, Cdc12p and Adf1p (Balasubramanian et al., 1998; Chang et al., 1997; Chen and Pollard, 2011). The assembly of contractile ring is promoted by the continuous polymerization of actin filaments in the ring (Courtemanche et al., 2016). As in higher eukaryotes, the ring contracts to drives the cleavage furrow ingression in fission yeast. This furrowing is also assisted by biosynthesis of the septum (Laplante et al., 2015; Mishra et al., 2013). The following cell separation, the terminal step of cytokinesis (for review see (Garcia Cortes et al., 2016; Sipiczki, 2007)), requires degradation of the septum (Cortes et al., 2002; Cortes et al., 2012; Liu et al., 1999; Munoz et al., 2013) as well as proper regulation of the turgor pressure (Atilgan et al., 2015; Proctor et al., 2012).

Although it remains a challenge to determine the free calcium concentration of live cells, the development of genetically encoded calcium indicators (GECI) over the last twenty years has made this task easier. Compared to the synthetic calcium probes, GECIs can be introduced into cells through exogenous expression, without requiring intrusive methods of probe-loading. This is particularly advantageous in genetically modifiable systems such as fission yeast that we used for this study. Although most GECIs still trail the chemical probes in their sensitivity, some of them such as GCaMP (Nagai et al., 2001), which we chose for this study, have come close. The single fluorophore sensor GCaMP consists of three domains: a circularly-permuted enhanced green-fluorescent protein (cp-EGFP), a calcium-binding calmodulin motif and a M13 peptide of human myosin-light chain kinase (MLCK). Binding of calcium to the calmodulin motif dissociates the M13 peptide from cp-EGFP, increases the fluorescence of GCaMP significantly

(Nakai et al., 2001). Over the years, modification of GCaMP sensors has substantially reduced their response time and enhanced the signal-to-noise ratio (Chen et al., 2013; Tian et al., 2009). We picked one of the most sensitive variants, GCaMP6s (Chen et al., 2013), to search for the potential calcium transients during cytokinesis of fission yeast.

Few studies have directly examined the intracellular calcium level of fission yeast, even though the calcium-signaling pathways has been studied extensively (Deng et al., 2006; Ma et al., 2011). Both calmodulin and calcineurin play a critical role in many cellular processes including cytokinesis (Takeda and Yamamoto, 1987; Yoshida et al., 1994). In this study we first explored the feasibility of GCaMP-based calcium imaging in fission yeast. For validation, we applied this method to both record the calcium homeostasis in unstimulated cells and capture the calcium transients triggered by osmotic stress in stimulated cells. We then examined the intracellular calcium level during cell division in our search for potential calcium transients. After the discovery of the cytokinetic calcium spikes, we also examined their significance to cytokinesis.

Results

Expression of the calcium indicator GCaMP

To quantify the intracellular calcium level, we expressed GCaMP from an endogenous locus in fission yeast. A strong ADH promoter drove the expression of GCaMP6s (referred to as GCaMP) at the *leu1* locus (Fig. 1A). To ensure that GCaMP localizes uniformly throughout the intracellular space for detection of free calcium, we determined its sub-cellular localization by tagging the C-terminus with another fluorescence protein mCherry. GCaMP-mCherry localized homogenously throughout the cytoplasm. It was also found in the nucleus where the reporter was slightly enriched compared to the cytoplasm (1.5 ± 0.1 folds, average ± standard deviation, n =

66), but GCaMP appeared to be excluded from the vacuoles (Fig. 1B). We concluded that the endogenously expressed GCaMP shall report the free calcium level throughout the intracellular space.

We next determined whether this calcium indicator perturbs any cellular function of fission yeast, a potential concern for a fluorescence reporter. The GCaMP expressing cells exhibited no apparent morphological defects (Fig. 1A). Their mitotic and septation indexes remained unchanged from that of the wild type (Fig. S1A-C). Lastly, these cells exhibited no hyper-sensitivity to either the presence of calcium or sorbitol, both of which perturb the intracellular calcium concentration, in the media (Fig. S1D). We concluded that expression of GCaMP doesn't produce any discernable artifacts in fission yeast.

To explore the potential correlation between cell division and the intracellular calcium level, we analyzed the GCaMP fluorescence among a large number of asynchronized cells. The length of a fission yeast cell can serve as an indicator for cell cycle (Mitchison and Nurse, 1985). Starting from a length of ~7μm after cytokinesis, a cell expands at its tips during interphase until stopping at ~14μm and entering mitosis. Overall, we found no correlation between the intracellular fluorescence and the length of a cell (Fig. 1C). The fluorescence remained low and varied very little among the GCaMP expressing cells regardless of their length. Only a small number of the cells (12%, n = 407) were significantly brighter (10% more) than the average. The length of these outliers followed a bimodal distribution with two peak fractions of 14 μm and 8 μm respectively (Fig. 1D), corresponding to the length of either a dividing cell or a separating cell. The existence of these outliers was the first hint that the intracellular calcium level of fission yeast may increase, albeit transiently, during cell division.

Validation of GCaMP-based calcium imaging

The utility of GCaMP as a calcium reporter for fission yeast had not been examined, even though it has been widely used in the studies of neuronal cells (Chen et al., 2013; Tian et al., 2009). As the first test, we inoculated the GCaMP expressing cells in YE media supplemented with calcium and examined their intracellular fluorescence with confocal fluorescence microscopy. Based on the bulk experiments (Deng et al., 2006), we expected this treatment to disrupt the calcium homeostasis, leading to elevated intracellular calcium level. Compared to those in YE, the average fluorescence of these cells indeed increased about three folds in the presence of 30mM $CaCl_2$ (Fig. 2A-B). Furthermore, time-lapse microscopy revealed that the intracellular fluorescence fluctuated with much higher frequency in the presence of the supplemented calcium (Fig. 2C-D and Supplemental Movie S1). We concluded that our GCaMP-based imaging method is capable of recording the homeostasis of intracellular calcium of fission yeast.

More critical to this study is to determine whether the GCaMP-based method is sensitive enough to capture calcium transients, a rapid change of intracellular calcium level that may last just seconds. Without a stimulus, the resting cells produced a very limited number of calcium transients, captured by our method (Fig. 2C). To trigger more consistent and predictable calcium transients, we shocked the cells with osmotic-stress, one of the best-known stimuli of calcium transients in yeast (Batiza et al., 1996; Denis and Cyert, 2002). We employed microfluidics to apply either hyper- or hypo-osmotic shocks while monitoring the intracellular fluoresce with time-lapse microscopy. First, the GCaMP expressing cells were trapped inside a microfluidic chamber infused continuously with YE media. Then a hyper-osmotic shock was applied by the infusion of YE media supplemented with sorbitol (up to 1.2M) (Fig. S2A). The fluorescence of these cells changed very little under such stress (Fig. S2B-C). In contrary, when we applied a hypo-osmotic shock by reducing the sorbitol concentration to zero in the media, we captured a

transient increase of the GCaMP fluorescence in all cells (Fig. 3A-C and Supplemental Movie S2). They started immediately after the cells re-expanded due to reduced extracellular osmolarity (Fig. 3B) and peaked at 2-3 mins after the osmotic shock (Fig. 3C). These calcium transients typically lasted no more than 2 mins. They were highly synchronized, but some heterogeneity existed among individual cells (Fig. 3A). Average amplitudes of these stress-induced calcium pikes were proportional to the strength of shocks (Fig. 3D). A maximal increase of five-fold can be triggered by dropping the sorbitol concentration from 1.2M to zero (Fig. 3D). We concluded that our GCaMP-based imaging can capture calcium transients in fission yeast.

Identification of calcium spikes during cytokinesis

Having validated our method of calcium imaging, we combined it with quantitative live microscopy to determine whether there are calcium transients in cytokinesis. We examined asynchronized cells to avoid the potential stress that usually accompanies the synchronization process such as temperature shift. To precisely align the time courses of calcium homeostasis during cytokinesis, we utilized an internal clock of cell-cycle, the separation of spindle pole bodies (SPB) (Fig. S3A) (Wu et al., 2003). The separation of SPBs is concomitant with the start of prometaphase, followed by metaphase and anaphase, which takes ~ 30 mins combined. Only few random calcium transients were captured during this period, among many dividing cells (n = 43). In contrast, at the beginning of telophase, the intracellular calcium level increased sharply and globally in the dividing cells (Fig. S3A-B). To determine whether this transient calcium increase, which we termed calcium spike, started at the time of furrowing as they did in the fish embryos (Chang and Meng, 1995b; Fluck et al., 1991), we more closely examined the temporal correlation between the calcium spikes and the contractile ring contraction (Fig. 4A-B). Very few calcium spikes were found during the assembly and maturation of the ring, which is not

surprisingly concurrent with metaphase and anaphase in fission yeast. In comparison, the intracellular calcium started to increase at the roughly same time as the contractile ring started to contract (Fig. 4C-D and Supplemental Movie S3). These spikes drove up the intracellular GCaMP fluorescence by up to 4 folds. They usually lasted more than two minutes, consisted of phases of fast rise and slow decay (Fig. S3C-D). The number of the spikes remained elevated, compared to that of the pre-contraction period, for the next 30 mins throughout the ring closure. The average intracellular calcium level only returned to the baseline when the ring closed completely. We concluded that the first cytokinetic calcium spikes accompanies the contraction of the contractile ring.

Next, we searched for potential calcium spikes during the cell separation, whose existence had been suggested by our earlier analysis (Fig. 1C). As the last step of cytokinesis, the separation starts from the end of the ring closure (Fig. 5A-B) till the appearance of the new ends of the daughter cells, lasting ~25 mins. Through time-lapse microscopy, we captured a second calcium spikes towards the end of cell separation. These spikes are highly synchronized, and they typically peaked 2 min after the end of cell separation (Fig. 5C-D and Supplemental Movie S4). Surprisingly, this calcium spike always appeared in just one daughter cell. It favored the one which inherited the new end of the mother cell over the other daughter cell by a ~2:1 ratio (Fig. S3G). Similar to the first calcium spikes, this second calcium spikes increased the intracellular GCaMP fluorescence by up to 4 folds (Fig. S3E-F). Although all of our observations so far were made of the cells grown in the rich YE5s media, similar two groups of cytokinetic calcium spikes were observed in dividing cells inoculated in the synthetic EMM5s media (Fig. S4A-B). We concluded that two groups of calcium spikes, concomitant with the furrow ingression and the end of cell separation respectively, accompany fission yeast cytokinesis.

Function of calcium spikes in cytokinesis

The close temporal correlation of fission yeast cytokinesis and the calcium spikes prompted us to investigate whether the spikes have any molecular role in cytokinesis. Alternatively, these calcium spikes could be just by-products of cytokinesis without a causal relationship. We decided to block the calcium spikes by removing the extracellular calcium temporarily through either chelation or growth in the calcium free media. First, 1-2mM of EGTA was added to the media to chelate the external calcium. This significantly reduced the number of outliers with higher than average intracellular calcium level in the population. It also decreased the number of cytokinetic calcium spikes that can be detected in the dividing cells (Fig. S4C-D and Supplemental Movie S5). Both results confirmed depletion of the calcium spikes by EGTA (Fig. 6A). Secondly, we inoculated the cells in the synthetic calcium-free media. The results were similar to that of EGTA treatment ((Fig. 6B and Fig. S4E-F), but slightly more spikes were detected in the calcium-free media, compared to EGTA supplemented media. We concluded that either EGTA or inoculation in calcium-free media can significantly deplete the cytokinetic calcium spikes.

We next determined whether blocking the calcium spikes has any effect on cytokinesis. Even with substantially reduced calcium spikes, mitosis of the dividing cells progressed without any delay (Fig. 6C and S5A-C). Surprisingly, the assembly plus maturation of the contractile ring was not delayed either (Fig. 6D-E). As a result, the contractile ring started to contract 30 mins after the separation of SPBs in these cells with few calcium spikes, not significantly different from that in untreated cells (Fig. 6D and 6E). However, the ring constricted much more slowly in these cells (Fig. 6F-G). 2mM EGTA reduced the contraction rate by almost half while the calcium free media by ~30% (Supplemental Movie S5). When we increased EGTA

concentration to 5mM, the contractile rings of most cells (90%, n = 30) disintegrated without completing the constriction (Fig. S5D). On the other hand, the cell separation proceeded without significant delay when the cytokinetic calcium spikes were depleted (Fig. 7A-B). However, more than one third (35 ± 5 %, n = 103) of dividing cells lysed immediately following the separation, when 2mM EGTA was present in the media (Fig. 7C). In most cases, both daughter cells lysed. Even more cells lysed in the presence of 5mM EGTA (Fig. S5E). Comparably, no lysis of separating cells was observed in the calcium-free media. We concluded that the cytokinetic calcium spikes are important to both promote the contraction of the contractile ring and maintain the integrity of separating cells.

Discussion

The calcium transient accompanying cytokinesis was first discovered in fish embryos (Fluck et al., 1991) but its existence beyond those large embryos had not been explored. It also remains ambiguous whether these transients have any role in regulating cytokinesis (Miller et al., 1993; Noguchi and Mabuchi, 2002; Snow and Nuccitelli, 1993). Using a novel calcium reporter, we searched for the potential calcium transients in fission yeast, a unicellular model organism that is about ten times smaller than the animal embryos. We discovered two intracellular calcium spikes during cytokinesis and determined their role in promoting the contractile ring contraction and the integrity of separating cells.

Novel GCaMP-based calcium imaging for fission yeast

To our knowledge, our study is the first to explore the feasibility of GCaMP-based calcium imaging in fission yeast. As adaptation of any fluorescence reporter in a living organism, the potential artifact is always a concern. Our study demonstrated that endogenous expression of GCaMP doesn't perturb cellular functions including cytokinesis of fission yeast. We picked

GCaMP6s, the most sensitive variant of GCaMP6 (Chen et al., 2013), for this work. The high sensitivity of this reporter enabled us to capture calcium spikes with relatively low frequency of image acquisition (no more than 1 frame/min), which is essential for reducing phototoxicity and photobleaching during our long-term (~ 3hrs) imaging of dividing cells *in vivo*.

In our study, the GCaMP-based calcium imaging exhibits two significant advantages over the synthetic probe-based approach. First, unlike the synthetic probes such as Calcium Green used in a previous study (Chang and Meng, 1995b), GCaMP can be expressed endogenously to maintain a constant intracellular concentration among the yeast cells. This, combined with quantitative microscopy, largely eliminated the need to correct for heterogeneity of the GCaMP fluorescence from individual cells. We took advantage of this system to identify a small number of outliers with elevated intracellular calcium level in a population. Secondly, the sub-cellular localization of this reporter can be easily determined. We did this through a tag of another fluorescence protein mCherry. This ensures that our GCaMP-based imaging can capture calcium transients throughout the cytoplasm and nucleus. In comparison, the localization of most synthetic probes is harder to determine. These probes often diffuse unevenly in the cytoplasm because of the localized injection. Overall, the GCaMP-based imaging shows great potential for studying calcium homeostasis during many cellular processes in the future.

The discovery of cytokinetic calcium spikes

Two independent approaches uncovered the cytokinetic calcium spikes in fission yeast. In addition to the time-lapse microscopy, we were able to examine hundreds of GCaMP expressing cells to identify a small number of outliers, which existence is consistent with the occurrence of two cytokinetic spikes. Comparably, most previous studies relied solely on the time-course recordings to identify the cytokinesis-specific calcium transients (Chang and Meng, 1995b;

Fluck et al., 1991; Noguchi and Mabuchi, 2002). Although no calcium spikes have been identified yet during budding yeast cytokinesis, Carbo et al. observed higher frequency of calcium bursts during G1 to S phase transition in synchronized cells (Carbo et al., 2017), which may be similar to the calcium spikes in the separating fission yeast cells.

The cytokinetic calcium spikes of fission yeast bear strong similarities to the calcium waves identified in some animal embryos. First, their temporal regulations are similar to each other. As in fission yeast, the first cytokinetic calcium wave of the animal embryos, the "furrowing wave" (Fluck et al., 1991), initiates just as the cleavage furrow starts to ingress (Chang and Meng, 1995b; Noguchi and Mabuchi, 2002). After the completion of the furrow ingression, the second "zipping wave", starts as the two daughter cells separate and move against each other (Fluck et al., 1991; Noguchi and Mabuchi, 2002). Secondly, the cytokinetic calcium transients of both animal embryos and fission yeast share similar kinetics. Both last for minutes, far longer than other known calcium transients including those fertilizing calcium waves (Jaffe and Creton, 1998). Both calcium transients travel at a relatively low speed. They travel at ~0.5 μm/s in the medaka fish embryo during cytokinesis (Fluck et al., 1991), about 50 times slower than those fertilizing waves (Jaffe, 1991). Similarly, it takes a few seconds for the cytokinetic calcium spikes to traverse the cytoplasm of relatively small fission yeast cells. The similarities between these cytokinetic calcium transients support the hypothesis that a temporary increase of intracellular calcium may represent a conserved regulatory mechanism of cytokinesis.

The key difference between the cytokinetic calcium transients of fission yeast and those of animal embryos is their sub-cellular localizations. In fission yeast, both calcium spikes propagate globally throughout the cytoplasm and nucleus. In contrast, the calcium waves of animal embryos are restricted to the cleavage furrow (Chang and Meng, 1995b; Fluck et al.,

1991) or its surrounding region (Noguchi and Mabuchi, 2002). This difference could be due to that the yeast calcium spikes can quickly diffuse away from the cleavage furrow in the relatively small fission yeast cells, obscuring their origin. In addition, the second calcium spikes occur asymmetrically in yeast while no such asymmetry was found of the second calcium wave in the animal embryos.

The cytokinetic calcium spikes of fission yeast most likely draw from both extracellular and internal-stored sources. Their dependence on external calcium was illustrated by the depletion of calcium spikes by the calcium-free media. On the other hand, the contribution from the intracellularly stored calcium is supported by the strong inhibitory effect of EGTA a calcium chelator. EGTA not only slowed down the contractile ring constriction as the calcium-free media did, but also triggered lysis of separating cells. The latter effect is most likely due to the chelation of the internally released calcium. In comparison, in animal embryos cytokinesis, the only source of calcium is from the internal store (Chang and Meng, 1995b; Miller et al., 1993). The influx of external calcium during cytokinesis could be mediated by tension-sensitive calcium channels on the plasma membrane (Fluck et al., 1991; Morris et al., 2019). In comparison, the release of internal calcium during the spikes could be mediated by the store-operated calcium release (SOCE) channels (Chan et al., 2016; Chan et al., 2015).

Potential role for the first cytokinetic calcium spike

We propose that the first calcium spikes promote the actomyosin ring constriction but they are not the trigger for the contraction. In comparison, the first cytokinetic “furrowing wave” of anima embryos has long been proposed as the trigger for the contractile ring contraction (Chang and Meng, 1995b; Fluck et al., 1991; Miller et al., 1993). In fission yeast, the ring contraction started without delay even in the presence of 2mM EGTA. Our proposed role for the first

calcium spike is consistent with our observation that the first spike usually peaks after the ring contraction starts.

The first calcium spike could promote the contraction through two potential mechanisms. First, it may increase the activity of type II myosin through phosphorylation of myosin regulatory light chain Rlc1p (Loo and Balasubramanian, 2008), as in the smooth muscle contraction. Secondly, the calcium spike may stimulate the biosynthesis of septum through activating the calcium-dependent phosphatase calcineurin (Cadou et al., 2013; Martin-Garcia et al., 2018; Yoshida et al., 1994). The septum formation plays an essential role in the elongation of the cleavage furrow in fission yeast (Proctor et al., 2012).

Potential role for the second cytokinetic calcium spike

We propose that the second calcium spike plays an important role in maintaining the integrity of separating cells. This is supported by our observation that many separating cells lysed in the presence of the calcium chelator EGTA when the calcium spikes were largely depleted. However, the second spike is not required for cell separation. No delay in cell separation was found in the presence of EGTA. The role of the second "zipping wave" found in animal embryos has remained largely unexplored since its discovery three decades ago (Fluck et al., 1991). It may promote the adhesion between two daughter cells in the frog embryos (Noguchi and Mabuchi, 2002) but there has been no supporting evidence. Our proposed role for the second cytokinetic calcium spike is also consistent with its temporal regulation. This spike consistently peaks only after the cell separation.

Two potential mechanisms may underlie the importance of the second cytokinetic spike. First, these calcium spikes could promote exocytosis to add new membrane at the cell division plane during the separation. Exocytosis during cytokinesis is essential for the integrity of

separating cells (Wang et al., 2016; Zhu et al., 2018). Secondly, these spikes may contribute to the regulation of intracellular osmolarity pressure during the separation, when a temporary increase of turgor pressure is required (Abenza et al., 2015; Proctor et al., 2012). This proposed mechanism will agree with the essential role of calcium spikes during cellular adaption to the osmotic stress (Batiza et al., 1996).

Overall, our work demonstrated that fission yeast, combined with time-lapse microscopy, could serve as an excellent model organism to study calcium transients during various cellular processes including cytokinesis and osmoregulation. Our discovery also demonstrates the surprising similarity between the regulation of intracellular calcium in fission yeast and that in animal embryos. Finally, we identified the potential roles of fission yeast cytokinetic calcium spikes that may have been conserved through evolution.

Materials and Method

Yeast genetics

We followed the standard protocols for yeast cell culture and genetics. Tetrads were dissected with a Spore+ micromanipulator (Singer, UK). Yeast cells were transformed with the lithium-acetate method. All the strains used in this study are listed (Table 1).

To construct the GCaMP expressing strain, we amplified the coding sequence from *pCMV-GCaMP6s* (Addgene, Plasmid #40753) through PCR using primers P589 and P590. The DNA fragment was subcloned into a previously described plasmid *pFA6a-KanMX6-Padh1-Tadh1* (Chen and Pollard, 2013). The GCaMP6s ORF, together with the Adh1 promoter and terminator, were integrated into the *leu1* locus through PCR-based homologous recombination using primers P413 and P414 (Bahler et al., 1998). The resulting strain was confirmed through both PCR using primers P589 and P416 and the Sanger sequencing using primer P668.

Fluorescence microscopy

For time-lapse microscopy, the cells were first inoculated in liquid YE5s media at 25°C for two days before they were harvested during the exponential growth phase at a density between $5*10^6$/ml to $1.0*10^7$/ml. 20 µl of the cell culture were spotted onto the glass-coverslip (#1.5) in a 10 mm petri dish (Cellvis, USA). The coverslip was pre-coated with 50µl of 50-100 µg/ml of lectin (Sigma, L2380) and allowed to dry for 3-4 hours in a 30°C incubator. After 10 min at room temperature, most cells attached to the coverslip in the petri dish. 2ml of YE5s media was then added to the dish before microscopy. When chelation of calcium in media is required, 2ml of YE5s supplemented with EGTA was added instead.

For the experiments in the calcium-free media, we prepared the synthetic EMM media by omitting $CaCl_2$ (100µM) and replacing calcium pantothenate (Vitamin B5) with sodium pantothenate (Cayman Chemical, Cat# NC1435671). The cells were first inoculated in YE5s media for 1 day, followed by another ~15 hours in EMM5s. After harvesting the exponentially growing cells, we washed them three times with the calcium-free media before proceeding to microscopy.

We employed a spinning disk confocal microscope for the time-lapse microscopy. The microscope is an Olympus IX71 unit equipped with a CSU-X1 spinning disk unit (Yokogawa, Japan). The motorized stage (ASI, USA) includes a Piezo Z Top plate for acquiring Z-series. The images were captured on an EMCCD camera (IXON-897, Andor) controlled by iQ3.0 (Andor). Solid-state lasers of 488 nm and 561 nm were used in the fluorescence microscopy, at power of no more than 2.5mW. Unless specified, we used a 60x objective lens (Olympus, Plan Apochromat, NA = 1.40). Typically, a Z-series of 8 slices at an interval of 1 µm was captured at each time point during the time-lapse microscopy. The temperature was maintained at ~22 ± 2°C

in a designated room for microscopy. To further minimize environmental variations, we typically imaged both control and experimental groups with randomized order in the same day.

For visualization of septum, we fixed the cells with 4% formaldehyde (EMS, USA) before staining them with 1 μg/ml of calcofluor white (Sigma, Cat# 18909). For visualization of nuclei, we fixed the cells with 70% cold ethanol before staining them with 1 μg/ml DAPI (Roche, Cat# 1023627001). To image fixed cells, we used an Olympus IX81 microscope equipped with a XM10 camera and a mercury lamp.

To apply osmotic stress, we used a CellASIC ONIX2 system (EMD Millipore), controlled by a desktop computer through the software ONIX (EMD Millipore). To trap cells in the imaging chamber of a microfluidics plate (Y04C), we injected the exponentially growing cell culture to the chamber at a pressure of 34.5 KPa for 2 mins, followed by a continuous infusion of YE5s media at a pressure of 10KPa for another 30 mins. To apply hyper-osmotic stresses, we injected YE5s plus sorbitol into the chamber at a pressure of 10KPa. Similarly, to apply hypo-osmotic stresses, we injected YE5s into the chamber at a pressure of 10KPa after the chamber had been equilibrated with a continuous infusion of YE5s plus sorbitol for 30 mins.

Image processing and analysis

We quantified the intracellular fluorescence of a GCaMP expressing cell as the total fluorescence intensity of the cell divided by its area. This value was used to represent the intracellular calcium level throughout the study. Cells were segmented manually, and their fluorescence intensities were quantified using average intensity projections of the Z-series. The intracellular fluorescence of the cells trapped in a microfluidics chamber was quantified by subtracting their combined fluorescence with the background fluorescence of the camera. Unless specified, we normalized the intracellular fluorescence of a cell against the baseline value, which is typically defined as the

average of the five lowest values recorded during a time course.

To measure the rate of the contractile ring closure, we determined the duration of the ring closure through analyzing the fluorescence kymograph of contractile ring. The closure rate was then calculated by dividing the initial circumference of the ring before the constriction by the duration. We used Image J (NIH) and custom-made macros for all the image analyses. The images were first corrected for X-Y drift using the Image J StackReg plug-in (Thevenaz et al., 1998) if necessary. Most plots were made with Kaleidagraph (Synergy, PA) except for the 3D plots which were made with OriginLab (OriginLab, MA). The figures were made with Canvas (ACDSee Systems).

Acknowledgement:

QC conceptualized the study, QC and AP designed and carried out the experiments, QC, AP and OS analyzed the data, QC and AP wrote the manuscript.

The authors would thank the other members of the Chen group, Debatrayee Sinha and Mamata Malla, for their help. They would also like to thank our colleagues at the University of Toledo Song-Tao Liu, William Taylor and Rick Komuniecki for suggestions. They would thank Dimitris Vavylonis (Lehigh University) and Ann Miller (University of Michigan) for thoughtful discussions. This work has been supported by the University of Toledo startup fund, NIGMS R15GM134496 and DeArce-Koch Memorial Fund to Q.C.

Table 1: The list of yeast strains

Strains	Genotype	Source
FY527	*h- leu1-32 ura4-D18 his3-D1 ade6-M216*	Lab stock
FY528	*h+ leu1-32 ura4-D18 his3-D1 ade6-M210*	Lab stock
QC-Y941	*h- leu1::kanMX6-Padh1-GCaMP6s*	This study
QC-Y989	*h- sad1-mCherry-NatMX6 kanMX6-GCaMP6s*	This study
QC-Y1004	*h+ rlc1-tdTomato-natMX6 kanMX6-GCaMP6s*	This study
QC-Y1068	*h- leu1::Padh1-GCaMP6s-mCherry*	This study
QC-Y274	*h- rlcl1-tdTomato sad1-mGFP*	Lab stock

Table 2: The list of DNA primers

Primers	Sequence
P413	*TTTGGGAGGTGAGGCTTCTACCGCTGATATTACTAAGGCTGTTGTTGAAGA ACTTGAAAAAATTTTGTAAGAATTCGAGCTCGTTTAAAC*
P414	*ATGCGACACAATTAATCAATAAAAATTAGGTCAAATCAAATCATATGAATT TATTCTACATTAAACCCTAGCGGCCGCCAGCTGAAGCTT*
P415	*CCTTCTCCTTCGTTATGGTTTG*
P589	*TTAATTAAC-ATGGGTTCTCATCATCATCATC*
P590	*GGCGCGCC-TCACTTCGCTGTCATCATTTGTAC*
P668	*CAGGGACACGGAAGAAGAAATTA*
P416	*TCATAAAGTTGAACGGATGTCG*

Figure legends

Figure 1. Expression and localization of GCaMP in fission yeast. (A) Bright-field (left) and fluorescence (right) micrographs of cells expressing GCaMP. Their intracellular fluorescence was low, except for one (white arrowhead). (B) The subcellular localization of GCaMP in fission yeast cells. Fluorescence micrographs of cells expressing GCaMP-mCherry. The insert shows the center slice of the Z-series of a representative cell (outlined in dashed lines, magnified). GCaMP-mCherry localized throughout the cytoplasm and nucleus, but it was excluded from the vacuoles. The intracellular fluorescence of mCherry was homogenous among all cells including those with elevated GCaMP fluorescence (white arrow heads). (C-D) Analysis of the fluorescence and the length of GCaMP expressing cells. The data was pooled from four independent experiments. (C) A scatter plot showing the relationship between intracellular fluorescence (normalized) of a cell and its length. There is no correlation between them. The fluorescence varied very little among the cells, regardless of their length. Only a few outliers exhibited elevated fluorescence compared to the average (blue line). The fluorescence intensity of a single cell was normalized against the mean value of all cells. (D) A histogram of the length of the outliers (10% brighter) from C. The black line represents the best fit of a bimodal distribution. The peak fractions are 8-9 μm and 14-15 μm respectively, closely matching that of either separated (7 μm) or dividing cells (14 μm).

Figure 2. GCaMP-based imaging of the intracellular calcium homeostasis. (A-B) Intracellular fluorescence of GCaMP expressing cells in YE5s media supplemented with 30mM $CaCl_2$. (A) Fluorescence micrographs (spectrum colored) of the cells in either YE5s (left) or YE5s supplemented with calcium (right). Bar represents the intensity scale. (B) Dot plot of the fluorescence intensities of the cells in either YE5s or YE5s supplemented with calcium ($n > 195$). Black line represents the average. Calcium increased the intracellular fluorescence of these

GCaMP expressing cells by ~3 folds. (C-D) Time-lapse microscopy of the GCaMP expressing cells. 3D-line plots show time courses of the fluorescence of twenty representative cells in either YE (C) or YE supplemented with 30mM $CaCl_2$ (D), recorded for one hour at 1 frame/min. Calcium triggered frequent fluctuations of the intracellular calcium level. Additionally, the GCaMP-based imaging captured a small number of spikes, marked by sharp and transient increase of the GCaMP fluorescence (arrows).

Figure 3 GCaMP-based imaging of the calcium spikes triggered by hypo-osmotic shock. (A-C) The GCaMP expressing cells, trapped in a microfluidic chamber, were equilibrated with YE5s supplemented with 1.2M sorbitol for 30 mins before the infusion of YE5s media without sorbitol (time zero). **(A)** Time-lapse micrographs of the cells in a representative field after the hypo-osmotic shock. Top: spectrum-colored fluorescence micrographs. Bottom: bright-field micrographs. The hypo-osmotic shock triggered a calcium spike in every cell. **(B)** Time-lapse micrographs of a representative cell after the shock. At +2 min, the calcium spike peaked, concomitant with the re-expansion of the tips (white arrowheads). **(C)** 3D-Line plots showing time courses of the GCaMP fluorescence of twenty cells before and after the osmotic shock. Fluorescence intensity is normalized against the mean intensity before the shock. **(D)** Average time courses of the fluorescence of the GCaMP expressing cells ($n > 100$) under various hypo-osmotic shocks. The amplitudes of the fluorescence increase are proportional to the strength of the shocks.

Figure 4. The first calcium spikes during the contractile ring contraction. (A) A schematic describing the average time course of the assembly, maturation and constriction of the contractile ring in the cells expressing GCaMP. The assembly and maturation took 31 ± 4 mins (average ± standard deviation, $n = 46$) while the constriction took 30 ± 3 mins ($n = 71$), consistent with the

previous values measured by us and others in the wild-type cells (Morris et al., 2019; Wu et al., 2003). **(B)** Time-lapse fluorescence micrographs of a dividing cell expressing GCaMP (spectrum-colored, top) and Rlc1p-tdTomato (gray, bottom). Numbers represent time in minutes after the contraction started. The interval between frames is 2 min. An intracellular spike initiated -2 min and peaked at 0 min before decaying slowly for the next 10 mins. **(C-D)** Intracellular calcium level during the assembly, maturation and constriction of the ring. **(C)** 3-D line plots showing the time courses of GCaMP fluorescence (n = 64). Most calcium spikes were concurrent with the start of the contraction, while some were also found during the ring closure. In comparison, very few occurred during the assembly and maturation. **(D)** Box plots of the GCaMP fluorescence of those cells shown in C. The number of observations made at each time point is shown. The average intracellular calcium level peaked at +2 min, after the contraction started.

Figure 5. The second calcium spikes during the cell separation. (A) A schematic describing the average time course of the separation of GCaMP expressing cells. Number represents time in minutes after the cell separation. The two daughter cells separated 25 ± 4 mins (n = 46) after the completion of the ring closure, consistent with the value measured in the wild type cells (Morris et al., 2019). **(B)** Time-lapse fluorescence micrographs of a representative cell expressing GCaMP (spectrum-colored, top). Interval = 1 min. The calcium spike initiated at 2 min and peaked at 3 min, followed by a slow decay in this cell. (C-D) Quantification of the calcium level during the separation. **(C)** 3-D line plots showing the time courses of the intracellular calcium level (n = 44). In most cells, the second calcium spike closely followed the cell separation. **(D)** Box plots of the GCaMP fluorescence of those cells shown in C. The number of observations made at each time point is shown. The average intracellular GCaMP fluorescence started to

increase at 0 min and peaked at +2 min.

Figure 6. The cytokinetic calcium spikes promote contraction of the actomyosin ring. (A-B) Blocking the calcium spikes through two approaches. Violin plots of the intracellular fluorescence of GCaMP expressing cells in (A) either YE or YE plus 2mM EGTA and (B) either regular or calcium-free EMM media. Box plots are showed as overlays. Both chelation by EGTA and inoculation in calcium-free media significantly reduced the number of outliers with elevated intracellular calcium level. **(C)** Time-lapse fluorescence micrographs of three cells in either YE5s (top), or YE5s supplemented with 1mM (middle), or 2mM EGTA (bottom). The cells expressed both Rlc1p-Tdtomato (red) and Sad1p-GFP (green). Number represents time after the separation of SPBs in minutes. Dash lines mark the outline of cells. **(D-E)** Scatter plots showing the duration of the ring assembly plus maturation (D) and the rate of the ring constriction (E) in the presence of EGTA. **(F-G)** Box plots showing durations of the assembly plus maturation (F) and the contraction rates in calcium-free media (G). Under either condition, the contractile ring constricted much more slowly but the assembly and maturation proceeded with delay.

Figure 7. The cytokinetic calcium maintains the integrity of separating cells. (A-B) Box plots showing the duration of the cell separation when the calcium spikes were largely blocked by either EGTA (A) or calcium-free media (B). Neither condition significantly delayed the separation. (C) Time-lapse micrographs of a separating cell in either YE or YE plus 2mM EGTA. In the presence of EGTA, 35% of daughter cells lysed immediately (asterisk) after the separation. Number represents time in minutes.

Supplemental Materials

Figure S1: GCaMP does not perturb cellular functions of fission yeast (related to Fig. 1). (A-C) Bar graphs comparing the wild-type cells that expressed GCaMP constitutively to those that did not. No significant differences were found in either their width (A), or their mitotic index

(B), or their septation index (C). (D) Ten-fold dilution series of both the wild-type (WT) and GCaMP expressing cells at various temperatures on either YE (top), or YE plus 25mM $CaCl_2$ (middle), or YE plus 1.2M sorbitol (bottom) plates. GCaMP did not inhibit growth under any of the conditions.

Figure S2: Hyper-osmotic shock doesn't calcium spikes (related to Fig. 3). (A) Time-lapse fluorescence micrographs (spectrum-colored) of GCaMP expressing cells in a microfluidic chamber. The chamber was infused with YE supplemented with either 0.6M (top) or 1.2M sorbitol (Bottom) at time zero. Numbers represent time in minutes after the shock. Unlike hypo-osmotic shocks, hyper-osmotic shocks didn't trigger synchronized intracellular calcium spikes. (B) 3D line plots showing time courses (n = 20) of intracellular GCaMP fluorescence during a hypo-osmotic shock. The chamber was infused with YE supplemented with 1.2M sorbitol. Few calcium spikes were found among these cells. (C) Average time courses of intracellular GCaMP fluorescence (n > 100) under different degrees of hyper-osmotic shock. Neither triggered synchronized calcium spikes.

Figure S3: Detection of calcium spikes during cytokinesis. (A-B) The intracellular calcium level increased during late mitosis. (A) Time-lapse fluorescence micrographs of a dividing cell. It expressed both Sad1-mCherry (red) and GCaMP (green). Number represents time after the SPB separation (arrowheads) in minutes. The interval between each frame is 4 mins. The intracellular calcium level peaked at +32 mins (asterisk), concomitant with the start of telophase. (B) A line plot showing the average time course of intracellular GCaMP fluorescence during mitosis. The intracellular calcium level increased towards the end of anaphase B, ~ 30 mins after the separation of SPBs and remained elevated for the next 30 mins. (C-D) The kinetics of cytokinetic calcium spikes. (C) Time-lapse micrographs of a cell expressing Rlc1p-tdTomato

(gray) and GCaMP (spectrum-colored) during a calcium spike. Left: a fluorescence micrograph showing the contracting ring at time zero. Number represent time in seconds. The interval between each frame is 3 secs. (D) A line plot showing quantification of the intracellular GCaMP fluorescence during the spike. The spike is consisted of a phase of fast rise followed by a slow decay.

Figure S4: Inhibition of the cytokinetic calcium spikes. 3-D line plots showing time courses of the fluorescence of the GCaMP expressing cells during either the ring closure (A, C and E) or the cell separation (B, D and F). (A-B) In EMM5s media. Two groups of calcium spikes were found in these cells during cytokinesis. (C-F) Depletion of the spikes through either chelation by EGTA (C-D) or inoculation in the calcium-free media (E-F). Under either condition, the cytokinetic calcium spikes were largely depleted from the dividing cells.

Figure S5: The calcium spikes promote both the contractile ring closure and the integrity of separating cells. (A) Time-lapse micrographs of a cell in either EMM5s (top) or the calcium-free EMM5s media (bottom). The cells expressed both Sad1-GFP (green) and Rlc1p-tdTomato (red). Number represents time in minutes after the separation of SPBs (time zero). The contraction took longer to complete (60 vs. 44 mins, underlined) in the cell in the calcium-free media, compared to the other one in EMM. (B-C) Mitosis progression when the calcium spikes were depleted. The line plots show the average time course of the distance between two SPBs of a dividing cell. The cloud represents the standard deviations. Either chelation by EGTA (B) or inoculation in the calcium-free media (C) didn't alter the mitotic progression significantly. (D-E) Cytokinesis in the presence of high concentration (5mM) of EGTA. Time-lapse micrographs of dividing cell in YE5s supplemented with 5mM EGTA. (D) A cell expressing both Sad1-GFP (green) and Rlc1p-tdTomato (red). The contractile ring failed to close completely before its

disintegration (arrowhead). (E) Top: Lysis of both daughter cells during the separation (asterisk). Interval = 4 mins. Bottom: Deformation of the septa (arrowhead) followed by lysis of one daughter cell. Interval = 2 mins. Number represent time in minutes.

Supplemental movies:

Movie S1: The calcium homeostasis of fission yeast reported by GCaMP-based imaging (related to Fig. 2). Time-lapse movie of GCaMP expressing cells in YE5s (left) or YE plus 30mM $CaCl_2$. Number indicates time in minutes. The intracellular fluorescence increased and fluctuated more in the presence of the supplemented calcium.

Movie S2: The calcium spikes of fission yeast captured by GCaMP-based imaging (related to Fig. 3). Time-lapse movie of the GCaMP expressing cells under continuous infusion of media at 10 KPa in a microfluidic chamber. At time zero, the infusing media was switched from YE5s supplemented with 1.2M sorbitol to YE5s to apply a hypo-osmotic shock. Left: fluorescence micrographs. Right: bright-field micrographs. Number indicted time in minutes. Upon the hypo-osmotic shock, the cells expanded immediately amid a transient spike of the intracellular fluorescence.

Movie S3: The first calcium spike during cytokinesis (related to Fig. 4). Time-lapse movie of a dividing cell expressing both GCaMP (green) and Rlc1p-tdTomato (red). Number indicated time in minutes after the ring contraction. This intracellular calcium spike initiated as the contraction started.

Movie S4: The second calcium spike during cytokinesis (related to Fig. 5). Time-lapse microscopy of a GCaMP expressing cell during the cell separation. Number indicates time in minutes after the separation. This intracellular calcium spike followed the separation, appearing in just one of the two daughter cells.

Movie S5: Cytokinesis with depleted calcium spikes (related to Fig. 6). Time-lapse microscopy of cells in either YE (left) or YE supplemented with 2mM EGTA (right). The cells expressed both GCaMP (green) and Rlc1p-tdTomato (red). In the presence of EGTA, the first calcium spike was not detectable, and the ring contraction took longer than that in YE media. Number represents time in minutes after initiation of the ring closure.

References

Abenza, J.F., E. Couturier, J. Dodgson, J. Dickmann, A. Chessel, J. Dumais, and R.E.C. Salas. 2015. Wall mechanics and exocytosis define the shape of growth domains in fission yeast. *Nature communications*. 6:8400.

Arnold, J.M. 1975. effect of calcium in cytokinesis as demonstrated with ionophore A231ß7. *Cytobiologie*. 11:1-9.

Atilgan, E., V. Magidson, A. Khodjakov, and F. Chang. 2015. Morphogenesis of the Fission Yeast Cell through Cell Wall Expansion. *Curr Biol*. 25:2150-2157.

Bahler, J., J.Q. Wu, M.S. Longtine, N.G. Shah, A. McKenzie, 3rd, A.B. Steever, A. Wach, P. Philippsen, and J.R. Pringle. 1998. Heterologous modules for efficient and versatile PCR-based gene targeting in Schizosaccharomyces pombe. *Yeast (Chichester, England)*. 14:943-951.

Batiza, A.F., T. Schulz, and P.H. Masson. 1996. Yeast respond to hypotonic shock with a calcium pulse. *J Biol Chem*. 271:23357-23362.

Cadou, A., A. Couturier, C. Le Goff, L. Xie, J.R. Paulson, and X. Le Goff. 2013. The Kin1 kinase and the calcineurin phosphatase cooperate to link actin ring assembly and septum synthesis in fission yeast. *Biol Cell*. 105:129-148.

Carbo, N., N. Tarkowski, E.P. Ipina, S.P. Dawson, and P.S. Aguilar. 2017. Sexual pheromone modulates the frequency of cytosolic Ca(2+) bursts in Saccharomyces cerevisiae. *Molecular biology of the cell*. 28:501-510.

Chan, C.M., J.T. Aw, S.E. Webb, and A.L. Miller. 2016. SOCE proteins, STIM1 and Orai1, are localized to the cleavage furrow during cytokinesis of the first and second cell division cycles in zebrafish embryos. *Zygote*. 24:880-889.

Chan, C.M., Y. Chen, T.S. Hung, A.L. Miller, A.M. Shipley, and S.E. Webb. 2015. Inhibition of SOCE disrupts cytokinesis in zebrafish embryos via inhibition of cleavage furrow deepening. *The International journal of developmental biology*. 59:289-301.

Chang, D.C., and C. Meng. 1995a. A localized elevation of cytosolic free calcium is associated with cytokinesis in the zebrafish embryo. *The Journal of cell biology*. 131:1539-1545.

Chang, D.C., and C.J.T.J.o.C.B. Meng. 1995b. A localized elevation of cytosolic free calcium is associated with cytokinesis in the zebrafish embryo. 131:1539-1545.

Chen, Q., and T.D. Pollard. 2013. Actin filament severing by cofilin dismantles actin patches and produces mother filaments for new patches. *Curr Biol*. 23:1154-1162.

Chen, T.W., T.J. Wardill, Y. Sun, S.R. Pulver, S.L. Renninger, A. Baohan, E.R. Schreiter, R.A. Kerr, M.B. Orger, V. Jayaraman, L.L. Looger, K. Svoboda, and D.S. Kim. 2013. Ultrasensitive fluorescent proteins for imaging neuronal activity. *Nature*. 499:295-300.

Clapham, D.E. 2007. Calcium signaling. *Cell*. 131:1047-1058.

Craig, R., R. Smith, and J. Kendrick-Jones. 1983. Light-chain phosphorylation controls the conformation of vertebrate non-muscle and smooth muscle myosin molecules. *Nature*. 302:436-439.

Deng, L., R. Sugiura, M. Takeuchi, M. Suzuki, H. Ebina, T. Takami, A. Koike, S. Iba, and T. Kuno. 2006. Real-time monitoring of calcineurin activity in living cells: evidence for two distinct Ca2+-dependent pathways in fission yeast. *Molecular biology of the cell*. 17:4790-4800.

Denis, V., and M.S. Cyert. 2002. Internal Ca(2+) release in yeast is triggered by hypertonic shock and mediated by a TRP channel homologue. *The Journal of cell biology*. 156:29-34.

Fluck, R.A., A.L. Miller, and L.F. Jaffe. 1991. Slow calcium waves accompany cytokinesis in

medaka fish eggs. *The Journal of cell biology*. 115:1259-1265.
Jaffe, L.F. 1991. The path of calcium in cytosolic calcium oscillations: a unifying hypothesis. *Proceedings of the National Academy of Sciences of the United States of America*. 88:9883-9887.
Jaffe, L.F., and R. Creton. 1998. On the conservation of calcium wave speeds. *Cell calcium*. 24:1-8.
Loo, T.H., and M. Balasubramanian. 2008. Schizosaccharomyces pombe Pak-related protein, Pak1p/Orb2p, phosphorylates myosin regulatory light chain to inhibit cytokinesis. *The Journal of cell biology*. 183:785-793.
Ma, Y., R. Sugiura, A. Koike, H. Ebina, S.O. Sio, and T. Kuno. 2011. Transient receptor potential (TRP) and Cch1-Yam8 channels play key roles in the regulation of cytoplasmic Ca2+ in fission yeast. *PLoS One*. 6:e22421.
Martin-Garcia, R., V. Arribas, P.M. Coll, M. Pinar, R.A. Viana, S.A. Rincon, J. Correa-Bordes, J.C. Ribas, and P. Perez. 2018. Paxillin-Mediated Recruitment of Calcineurin to the Contractile Ring Is Required for the Correct Progression of Cytokinesis in Fission Yeast. *Cell reports*. 25:772-783 e774.
Miller, A.L., R.A. Fluck, J.A. McLaughlin, and L.F. Jaffe. 1993. Calcium buffer injections inhibit cytokinesis in Xenopus eggs. *Journal of cell science*. 106 (Pt 2):523-534.
Mitchison, J.M., and P. Nurse. 1985. Growth in cell length in the fission yeast Schizosaccharomyces pombe. *Journal of cell science*. 75:357-376.
Morris, Z., D. Sinha, A. Poddar, B. Morris, and Q. Chen. 2019. Fission yeast TRP channel Pkd2p localizes to the cleavage furrow and regulates cell separation during cytokinesis. *Molecular biology of the cell*. 30:1791-1804.
Nagai, T., A. Sawano, E.S. Park, and A. Miyawaki. 2001. Circularly permuted green fluorescent proteins engineered to sense Ca2+. *Proceedings of the National Academy of Sciences of the United States of America*. 98:3197-3202.
Nakai, J., M. Ohkura, and K. Imoto. 2001. A high signal-to-noise Ca(2+) probe composed of a single green fluorescent protein. *Nat Biotechnol*. 19:137-141.
Nishimura, J., R.A. Khalil, J.P. Drenth, and C. van Breemen. 1990. Evidence for increased myofilament Ca2+ sensitivity in norepinephrine-activated vascular smooth muscle. *The American journal of physiology*. 259:H2-8.
Noguchi, T., and I. Mabuchi. 2002. Localized calcium signals along the cleavage furrow of the Xenopus egg are not involved in cytokinesis. *Molecular biology of the cell*. 13:1263-1273.
Proctor, S.A., N. Minc, A. Boudaoud, and F. Chang. 2012. Contributions of turgor pressure, the contractile ring, and septum assembly to forces in cytokinesis in fission yeast. *Curr Biol*. 22:1601-1608.
Scholey, J.M., K.A. Taylor, and J. Kendrick-Jones. 1980. Regulation of non-muscle myosin assembly by calmodulin-dependent light chain kinase. *Nature*. 287:233-235.
Snow, P., and R. Nuccitelli. 1993. Calcium buffer injections delay cleavage in Xenopus laevis blastomeres. *The Journal of cell biology*. 122:387-394.
Takeda, T., and M. Yamamoto. 1987. Analysis and in vivo disruption of the gene coding for calmodulin in Schizosaccharomyces pombe. *Proc Natl Acad Sci U S A*. 84:3580-3584.
Thevenaz, P., U.E. Ruttimann, and M. Unser. 1998. A pyramid approach to subpixel registration based on intensity. *IEEE Trans Image Process*. 7:27-41.
Tian, L., S.A. Hires, T. Mao, D. Huber, M.E. Chiappe, S.H. Chalasani, L. Petreanu, J. Akerboom, S.A. McKinney, E.R. Schreiter, C.I. Bargmann, V. Jayaraman, K. Svoboda, and L.L.

Looger. 2009. Imaging neural activity in worms, flies and mice with improved GCaMP calcium indicators. *Nat Methods*. 6:875-881.

Wang, N., I.J. Lee, G. Rask, and J.Q. Wu. 2016. Roles of the TRAPP-II Complex and the Exocyst in Membrane Deposition during Fission Yeast Cytokinesis. *PLoS biology*. 14:e1002437.

Wu, J.Q., J.R. Kuhn, D.R. Kovar, and T.D. Pollard. 2003. Spatial and temporal pathway for assembly and constriction of the contractile ring in fission yeast cytokinesis. *Developmental cell*. 5:723-734.

Yoshida, T., T. Toda, and M. Yanagida. 1994. A calcineurin-like gene ppb1+ in fission yeast: mutant defects in cytokinesis, cell polarity, mating and spindle pole body positioning. *Journal of cell science*. 107 (Pt 7):1725-1735.

Zhu, Y.H., J. Hyun, Y.Z. Pan, J.E. Hopper, J. Rizo, and J.Q. Wu. 2018. Roles of the fission yeast UNC-13/Munc13 protein Ync13 in late stages of cytokinesis. *Molecular biology of the cell*. 29:2259-2279.

Figure 1

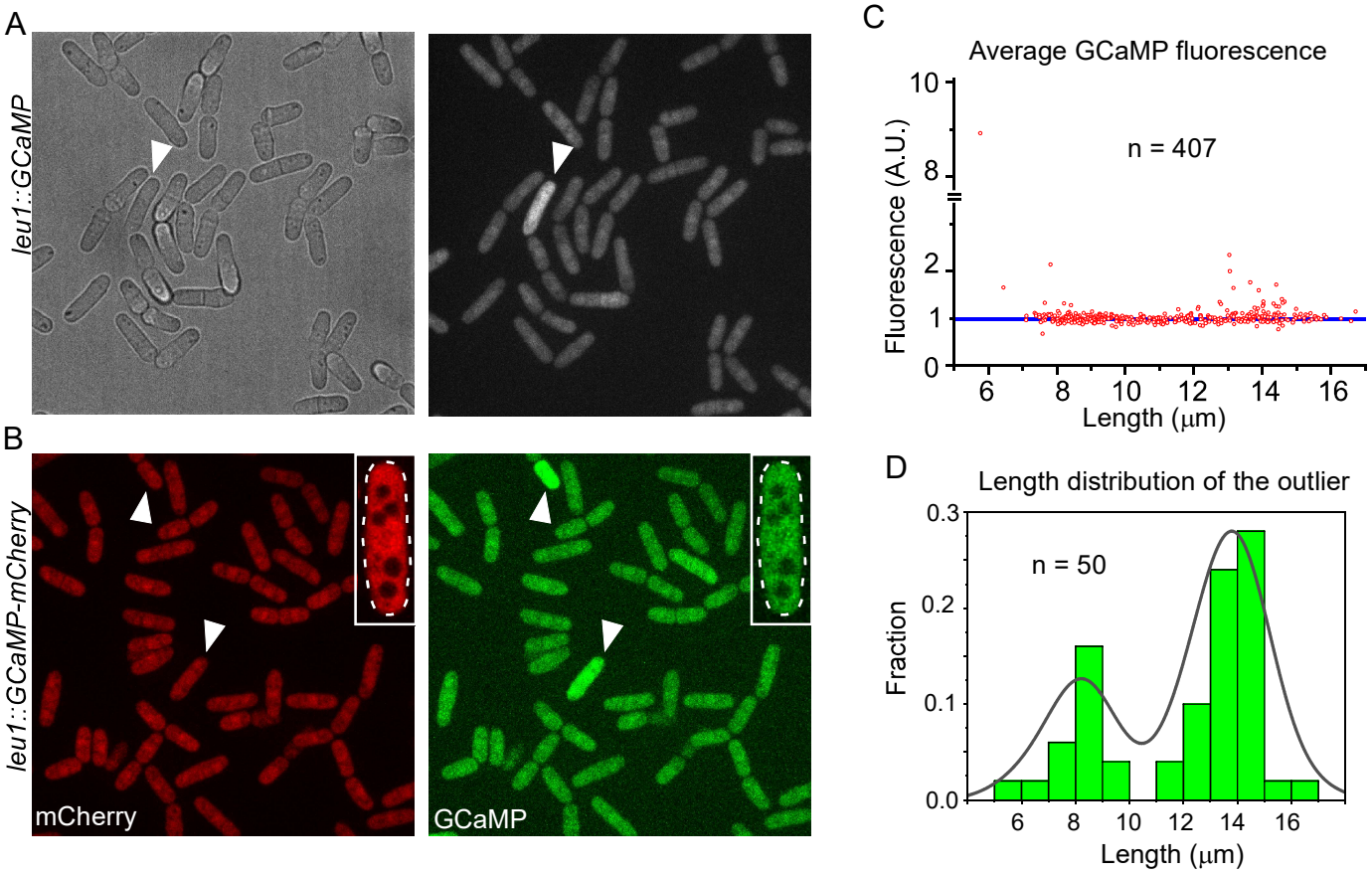
A
leu1::GCaMP
B
leu1::GCaMP-mCherry
mCherry
GCaMP
C
Average GCaMP fluorescence
n = 407
Fluorescence (A.U.)
Length (μm)
D
Length distribution of the outlier
n = 50
Fraction
Length (μm)

Figure 2

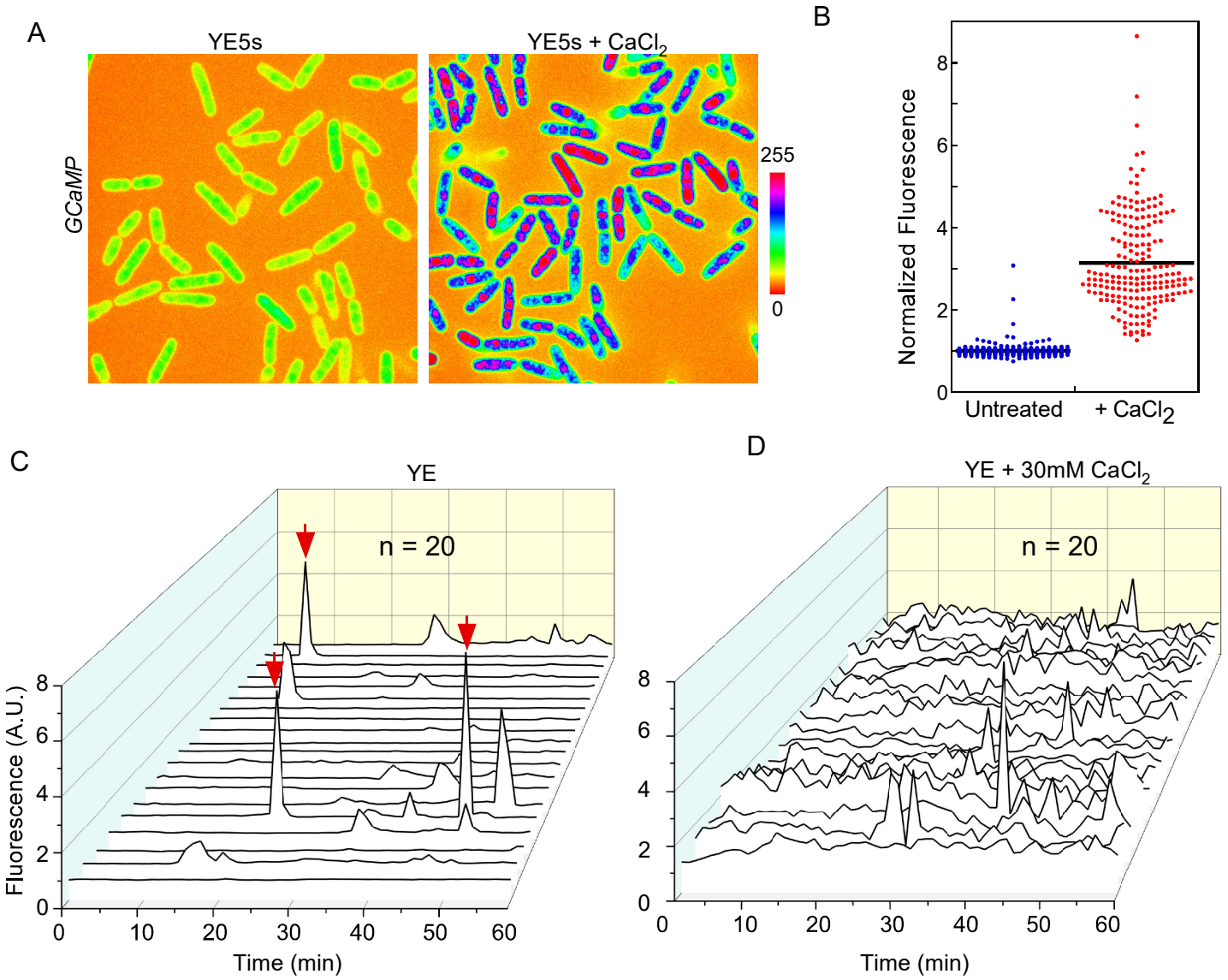
A
YE5s
YE5s + CaCl2
GCaMP
255
0
B
Normalized Fluorescence
Untreated
+ CaCl2
C
YE
n = 20
Fluorescence (A.U.)
Time (min)
D
YE + 30mM CaCl2
n = 20
Time (min)

Figure 3

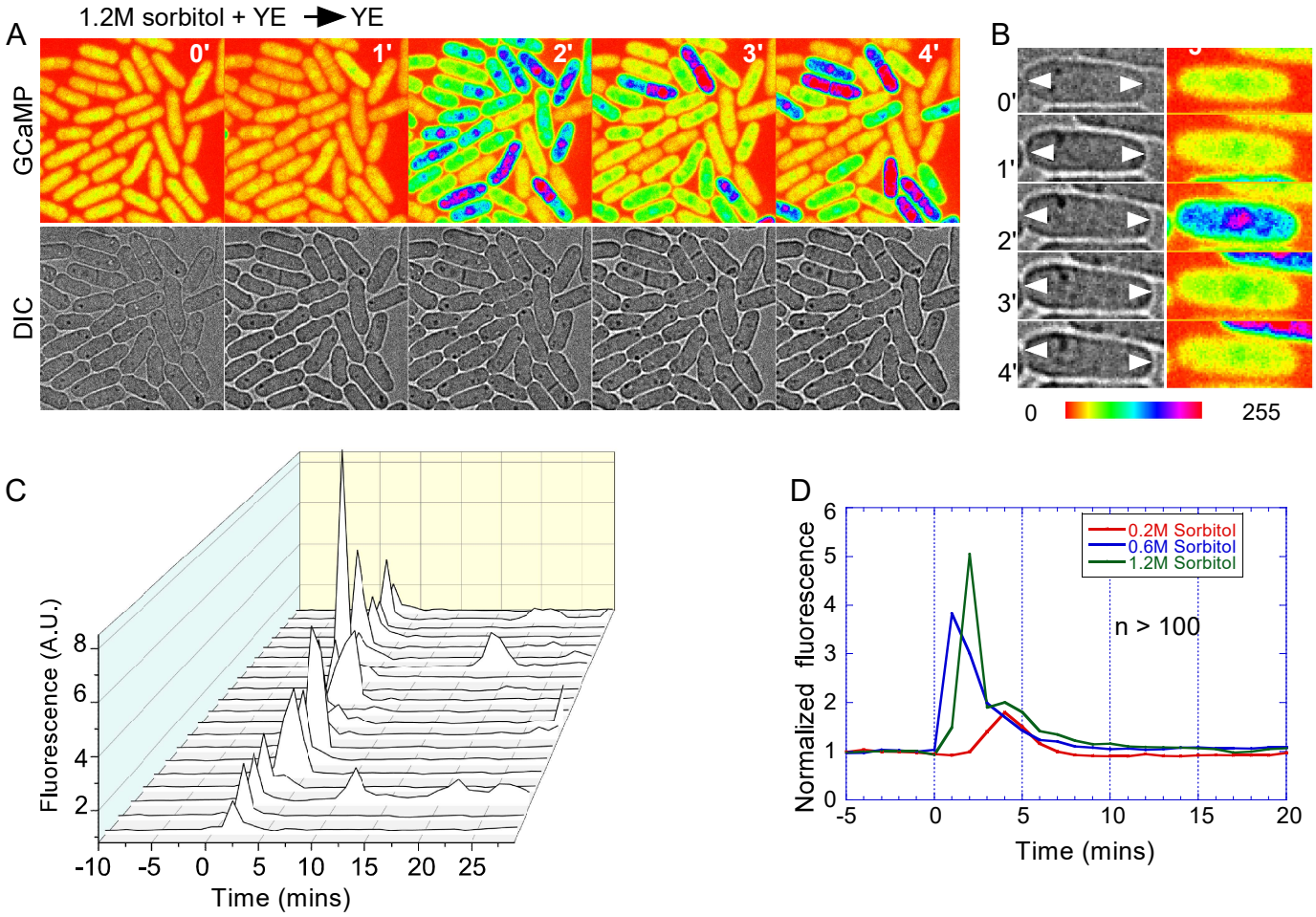
A
1.2M sorbitol + YE
YE
0'
1'
2'
3'
4'
GCaMP
DIC
B
0'
1'
2'
3'
4'
0
255
C
Fluorescence (A.U.)
Time (mins)
D
0.2M Sorbitol
0.6M Sorbitol
1.2M Sorbitol
n > 100
Normalized fluorescence
Time (mins)

Figure 4

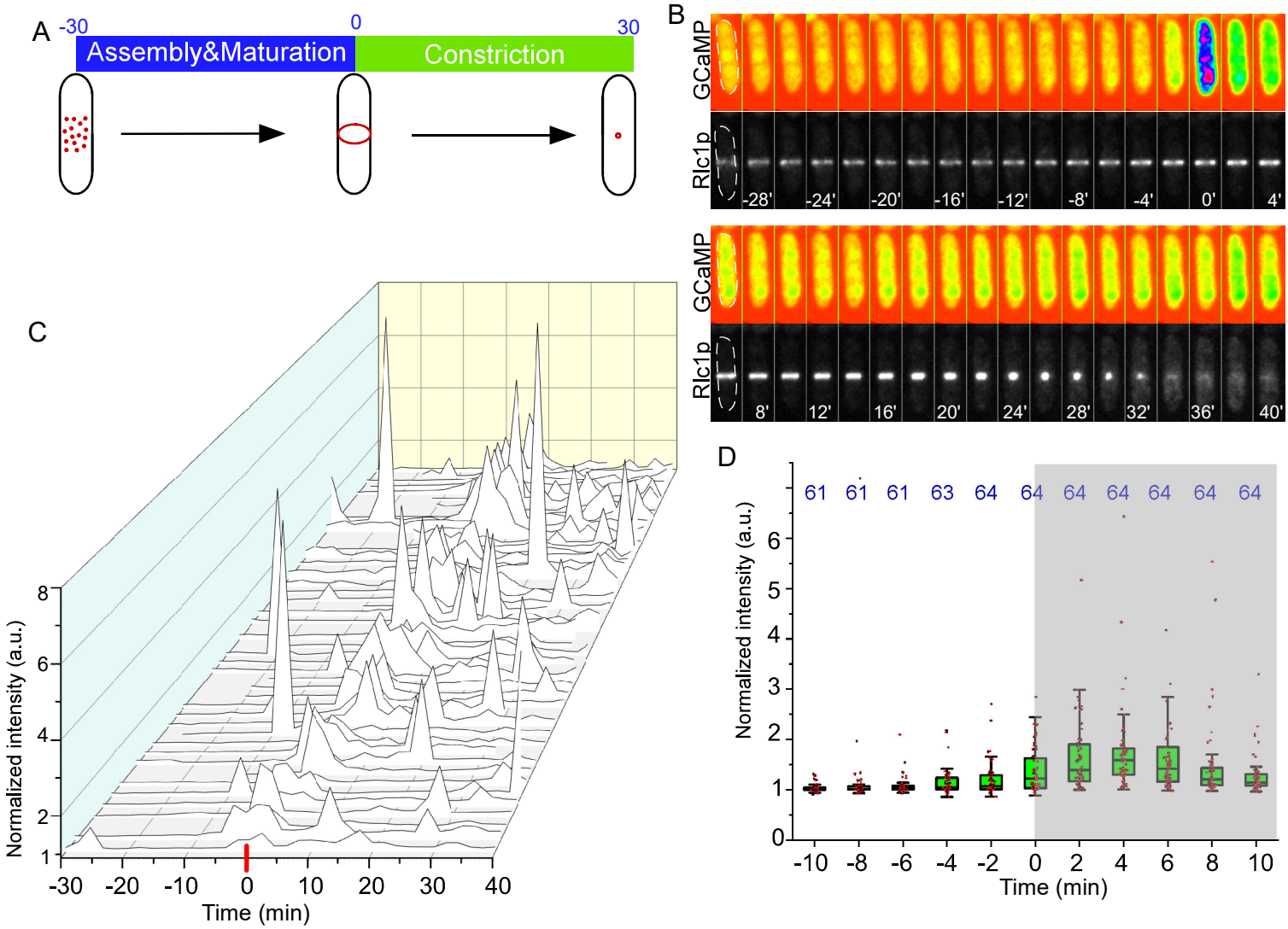
A
-30
0
30
Assembly&Maturation
Constriction
B
GCaMP
Rlc1p
-28'
-24'
-20'
-16'
-12'
-8'
-4'
0'
4'
GCaMP
Rlc1p
8'
12'
16'
20'
24'
28'
32'
36'
40'
C
Normalized intensity (a.u.)
Time (min)
D
61 61 61 63 64 64 64 64 64 64 64
Normalized intensity (a.u.)
Time (min)

Figure 5

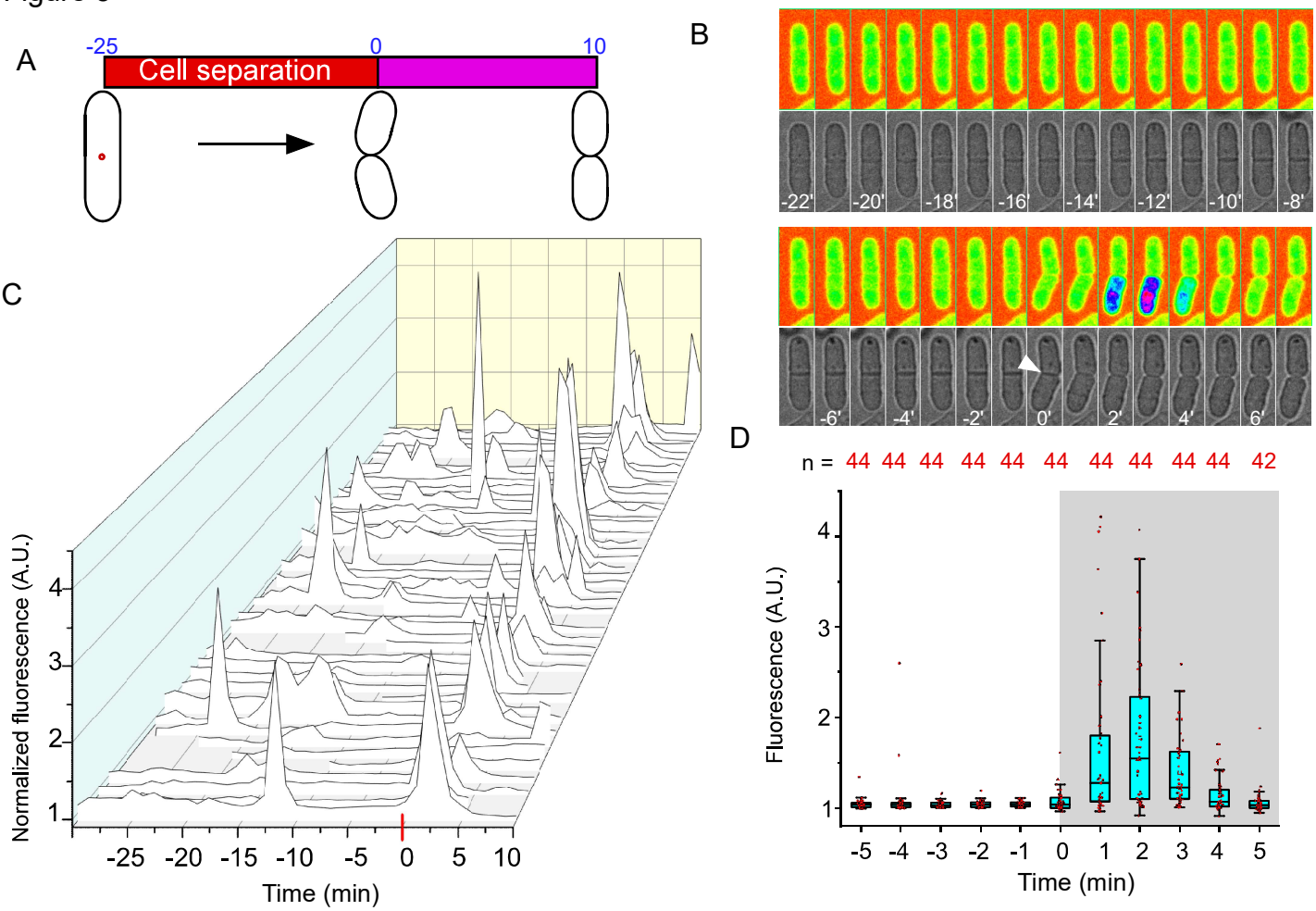
A
-25
0
10
Cell separation
B
-22'
-20'
-18'
-16'
-14'
-12'
-10'
-8'
-6'
-4'
-2'
0'
2'
4'
6'
C
Normalized fluorescence (A.U.)
1
2
3
4
-25 -20 -15 -10 -5 0 5 10
Time (min)
D
n = 44 44 44 44 44 44 44 44 44 44 42
Fluorescence (A.U.)
1
2
3
4
-5 -4 -3 -2 -1 0 1 2 3 4 5
Time (min)

Figure 6

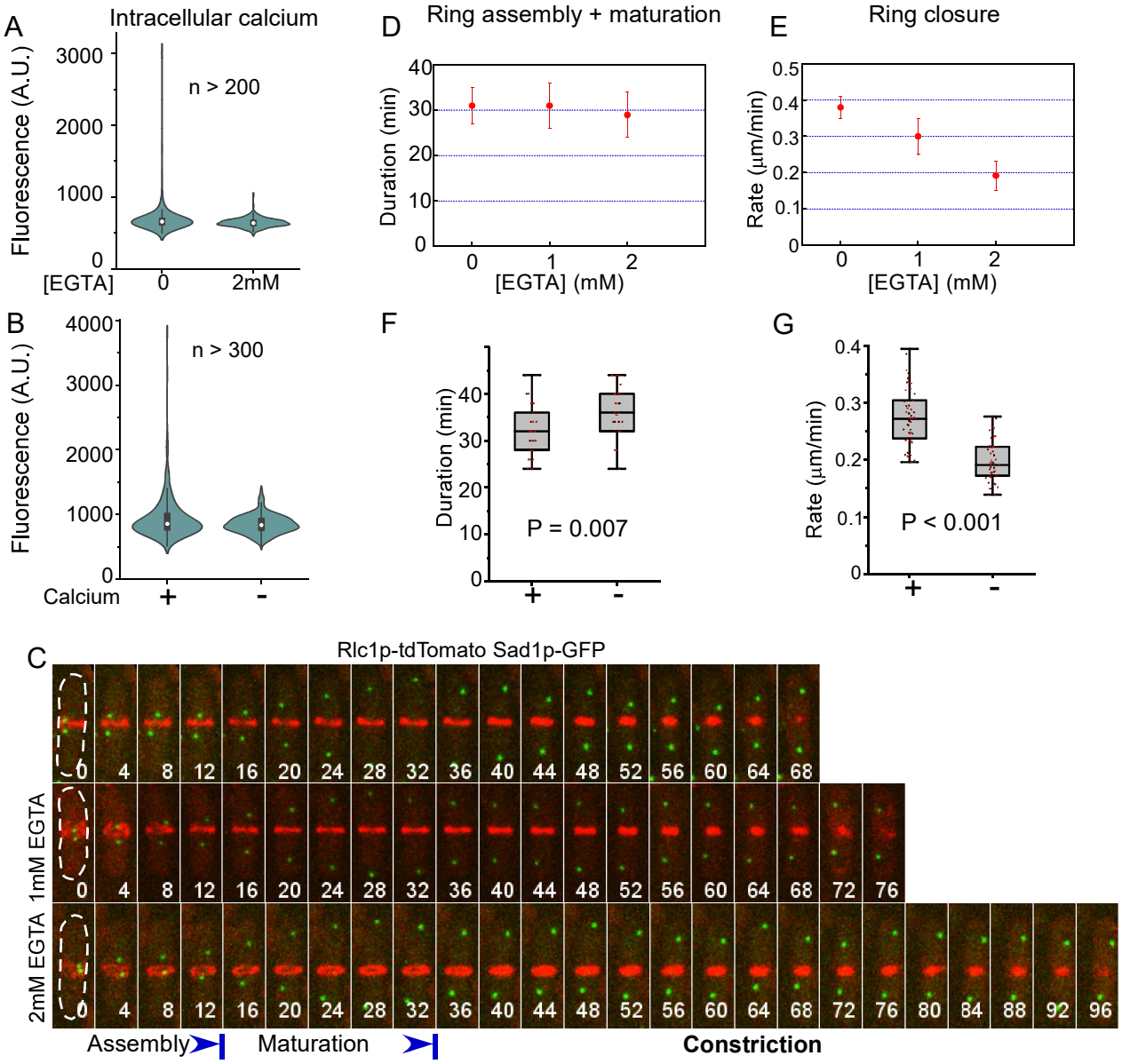
A
Intracellular calcium
Fluorescence (A.U.)
n > 200
[EGTA]
0
2mM
B
n > 300
Calcium
+
-
D
Ring assembly + maturation
Duration (min)
[EGTA] (mM)
E
Ring closure
Rate (µm/min)
F
P = 0.007
G
P < 0.001
C
Rlc1p-tdTomato Sad1p-GFP
1mM EGTA
2mM EGTA
Assembly
Maturation
Constriction

Figure 7

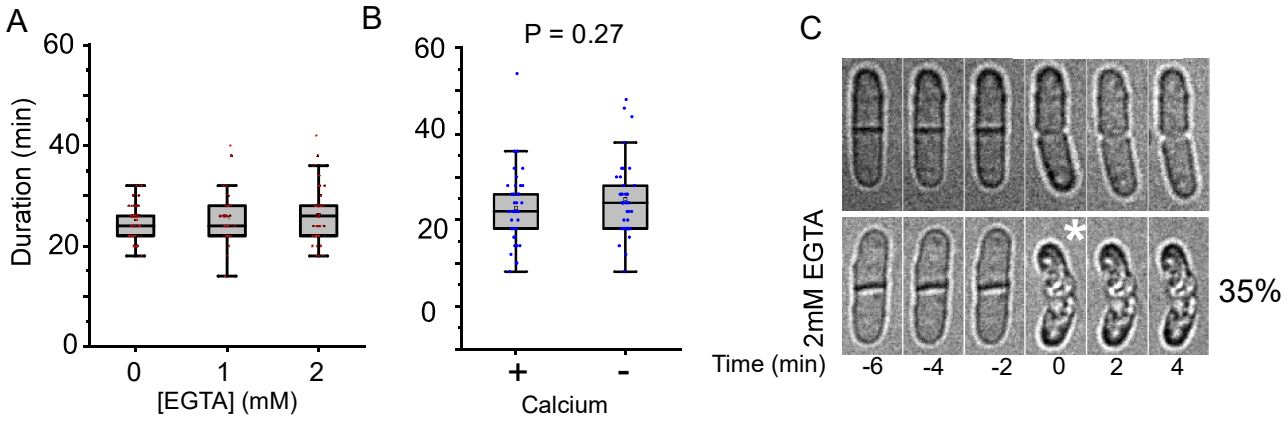
A
60
40
20
0
Duration (min)
0
1
2
[EGTA] (mM)
B
P = 0.27
60
40
20
0
+
-
Calcium
C
2mM EGTA
*
35%
Time (min)
-6
-4
-2
0
2
4

Figure S1

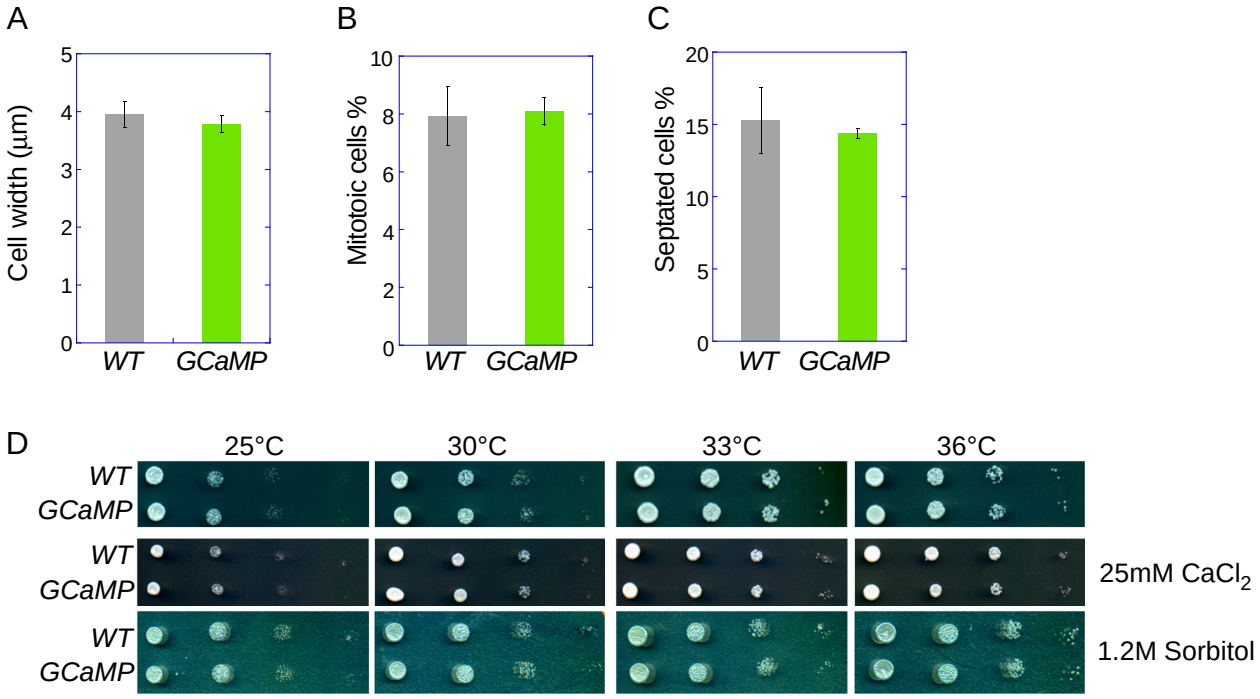
A
Cell width (µm)
0
1
2
3
4
5
WT
GCaMP
B
Mitotoic cells %
0
2
4
6
8
10
WT
GCaMP
C
Septated cells %
0
5
10
15
20
WT
GCaMP
D
25°C
30°C
33°C
36°C
WT
GCaMP
WT
GCaMP
25mM CaCl2
WT
GCaMP
1.2M Sorbitol

Figure S2

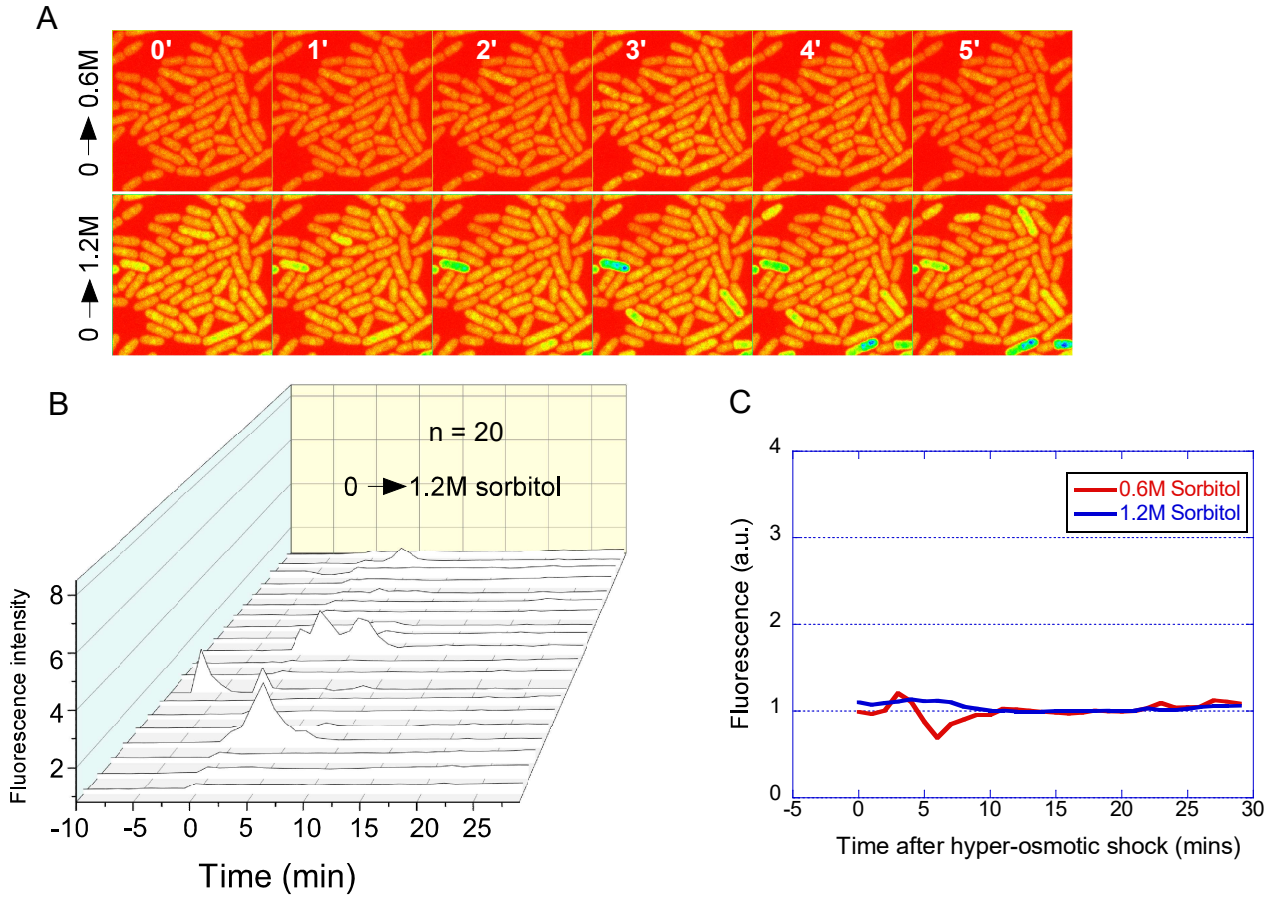
A
0'
1'
2'
3'
4'
5'
0 → 0.6M
0 → 1.2M
B
n = 20
0 → 1.2M sorbitol
Fluorescence intensity
Time (min)
C
0.6M Sorbitol
1.2M Sorbitol
Fluorescence (a.u.)
Time after hyper-osmotic shock (mins)

Figure S3

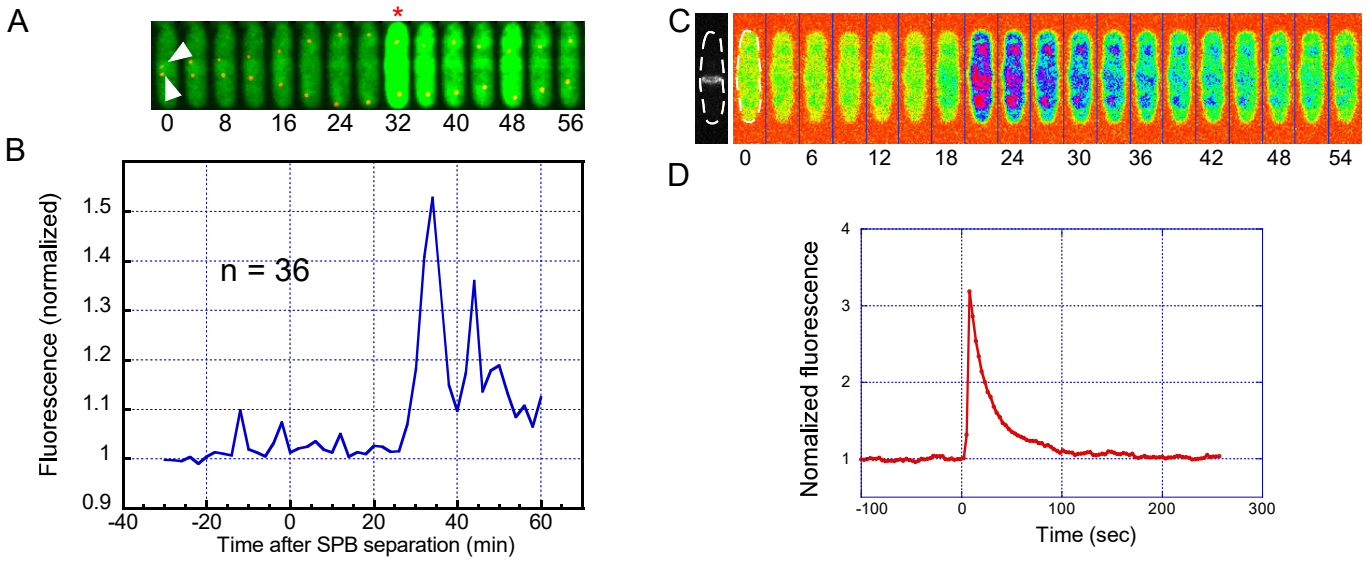
A
*
0
8
16
24
32
40
48
56
B
n = 36
Fluorescence (normalized)
1.5
1.4
1.3
1.2
1.1
1
0.9
-40
-20
0
20
40
60
Time after SPB separation (min)
C
0
6
12
18
24
30
36
42
48
54
D
Nomalized fluorescence
4
3
2
1
-100
0
100
200
300
Time (sec)

Figure S4

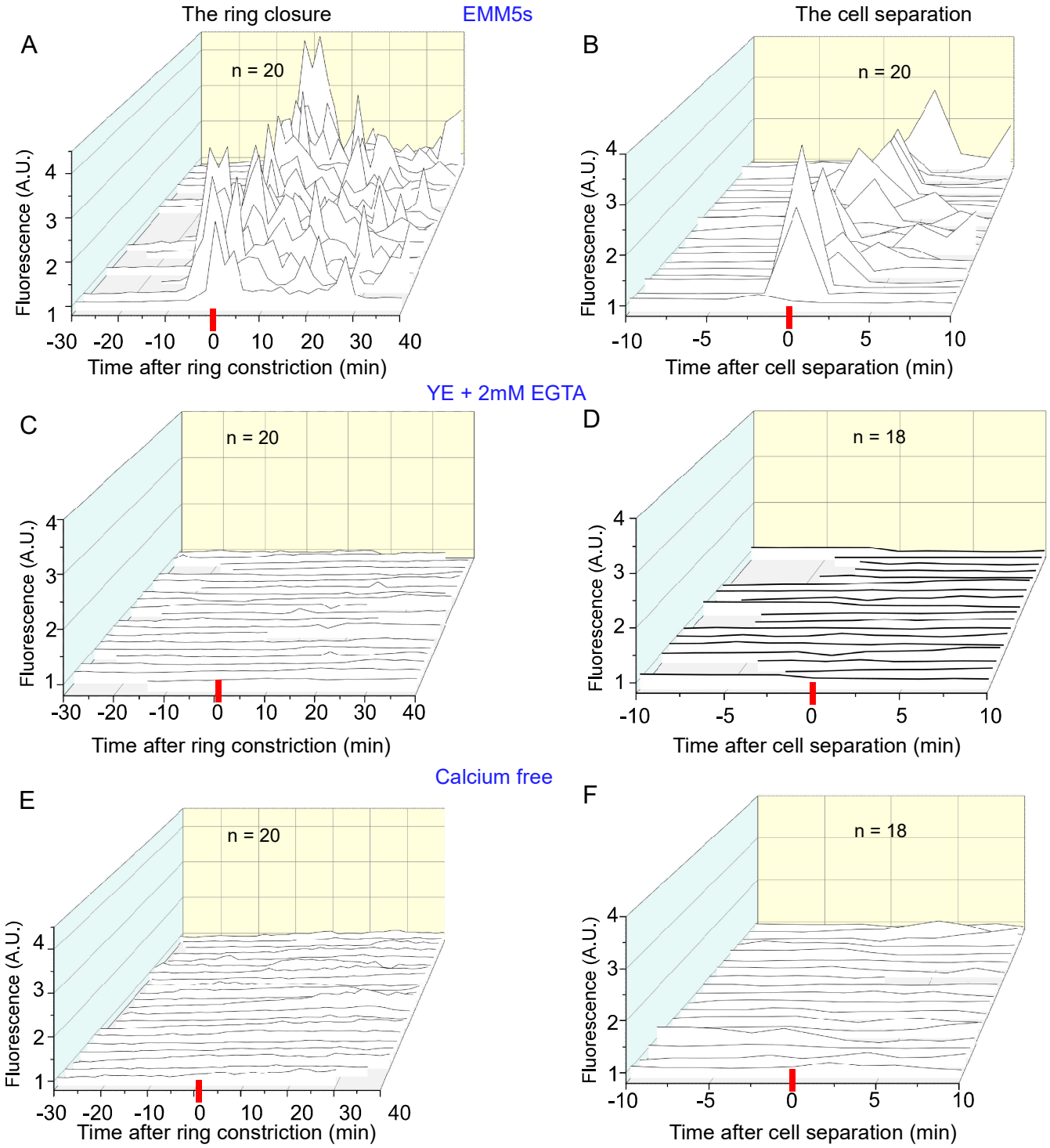
The ring closure
EMM5s
The cell separation
A
n = 20
B
n = 20
Fluorescence (A.U.)
Time after ring constriction (min)
Time after cell separation (min)
YE + 2mM EGTA
C
n = 20
D
n = 18
Calcium free
E
n = 20
F
n = 18

Figure S5

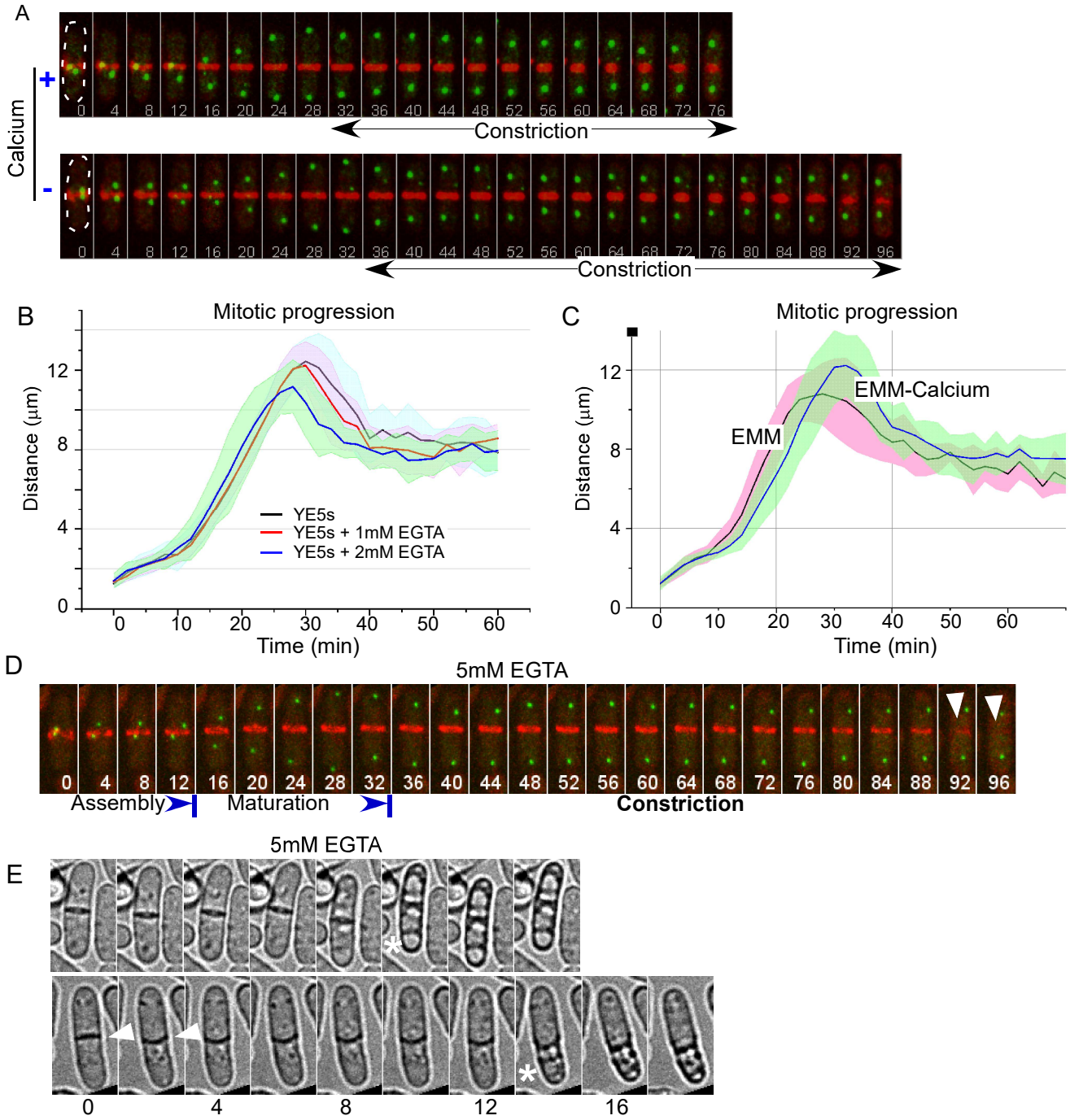
A
Calcium
+
-
0 4 8 12 16 20 24 28 32 36 40 44 48 52 56 60 64 68 72 76
Constriction
0 4 8 12 16 20 24 28 32 36 40 44 48 52 56 60 64 68 72 76 80 84 88 92 96
Constriction
B
Mitotic progression
Distance (μm)
Time (min)
YE5s
YE5s + 1mM EGTA
YE5s + 2mM EGTA
C
Mitotic progression
Distance (μm)
Time (min)
EMM
EMM-Calcium
D
5mM EGTA
0 4 8 12 16 20 24 28 32 36 40 44 48 52 56 60 64 68 72 76 80 84 88 92 96
Assembly
Maturation
Constriction
E
5mM EGTA
0
4
8
12
16